On the Nullity of Altans and Iterated Altans

Nino Bašić 1,2,3,* and Patrick W. Fowler 4,*

¹FAMNIT, University of Primorska, Koper, Slovenia ²IAM, University of Primorska, Koper, Slovenia ³Institute of Mathematics, Physics and Mechanics, Ljubljana, Slovenia ⁴Department of Chemistry, University of Sheffield, Sheffield S3 7HF, UK

March 14, 2022

Abstract

Altanisation (formation of the altan of a parent structure) originated in the chemical literature as a formal device for constructing generalised coronenes from smaller structures. The altan of graph G, denoted $\mathfrak{a}(G,H)$, depends on the choice of attachment set H (a cyclic h-tuple of vertices of G). From a given pair (G,H), the altan construction produces a pair (G',H'), where H' is called the induced attachment set. Repetition of the construction, using at each stage the attachment set induced in the previous step, defines the iterated altan. Here, we prove sharp bounds for the nullity of altan and iterated altan graphs based on a general parent graph: for any attachment set with odd h, nullities of altan and parent are equal; for any h and all $k \geq 1$, the k-th altan has the same nullity as the first; for any attachment set with even h, the nullity of the altan exceeds the nullity of the parent graph by one of the three values $\{0,1,2\}$. The case of excess nullity 2 has not been noticed before; for benzenoids with the natural attachment set consisting of the CH sites, it occurs first for a parent structure with 5 hexagons. On the basis of extensive computation, it is conjectured that in fact no altan of a convex benzenoid has excess nullity 2.

Keywords: Altan, attachment set, nullity, iterated altan, chemical graph, benzenoid, patch, non-bonding orbital.

Math. Subj. Class. (2020): 05C50, 15A18, 05C92

1 Introduction

Aromaticity has been an influential concept in chemistry for a century and a half, and despite difficulties with precise definition is still invoked routinely in qualitative explanation of stability, reactivity and magnetic response of conjugated systems [1–5]. On the widely accepted magnetic criterion, aromaticity is defined by the ability of a system to sustain *ring currents* (circulations of (π) electrons) induced by a perpendicular external magnetic field [6–9], where a multi-centre π current with diatropic/paratropic sense implies aromaticity/anti-aromaticity and absence of current implies non-aromaticity. The prediction of patterns of ring current

and design of carbon nanostructures with specific magnetic properties are subjects of active research [10,11]. One strategy for design of carbon nanostructures that should support concentric currents is based on the venerable annulene-within-an-annulene model [12–15], which predicts combinations of inner and outer currents on concentric cycles connected by 'spoke' bonds. Depending on the lengths of inner and outer circuits, and the strength of the spoke coupling between them, any of the four combinations of diatropic and paratropic current may appear [13,16–18]. As with many chemical models, this approach gives a rule of thumb rather than a rigorous prediction [19], but it can serve as a starting point for more detailed explanations.

A development from this earlier picture is the formal strategy of 'altanisation' in which a central carbon framework is surrounded by an **an**nulene perimeter in which carbon centres with two and three carbon neighbours **alternate** [10, 20, 21]. The *altan* concept has spawned a sizeable quantum chemical literature, in which the construction is used to generate systems (often hypothetical) for which properties can be calculated with empirical, semi-empirical or *ab initio* methods [17,22–31]. Interest has centred on creating systems with unusual paratropic perimeter currents [18] or with unusual dependence of outer currents on the total charge [31].

In qualitative theories of electronic structure in organic chemistry, there is a conceptual split between localised and delocalised descriptions, based respectively on Kekulé structures (perfect matchings) or the balance of bonding, non-bonding and anti-bonding molecular orbitals (eigenvectors corresponding to positive, zero and negative eigenvalues of the adjacency matrix). One important quantity is the *nullity* of the graph – the multiplicity of the zero eigenvalue, or in chemical terms, the number of non-bonding π molecular orbitals (NBMOs). The altan construction has inspired mathematical investigations of matchings and spectra [32–35]: altans may be Kekulean (have a perfect matching) or not, and their graphs may be singular (have at least one zero eigenvalue of the adjacency matrix) or not.

In the Hückel model of unsaturated carbon frameworks, the number of NBMOs [36] has consequences for stability, reactivity and magnetic properties. Nullity is also of interest in the context of *graph energy* [37–39]. For the general theory of graph spectra, the reader may consult standard references [40–44], and for a survey on nullity see [45].

Nullity has been studied for altans using a mixture of formal theorems and empirical observations on small sets of examples, and a certain amount of confusion about the limits on altan nullity has arisen as a result. We aim to clarify the situation here. Specifically, in the present paper, we build on established mathematical results [32,33] to derive the precise relationship between the nullity of the altan and the parent graph, and between nullities of first and subsequent iterated altans. Some previously unsuspected cases of a higher increase in nullity on first altanisation are detected. These occur for surprisingly small chemical examples.

2 Preliminaries

2.1 The altan construction

In this section we give a formal graph-theoretical definition of the altan of a graph G and develop some useful concepts. We follow Gutman's definitions [33] with some variations in terminology and notation. The primary object of our study is the pair (G, H) where G is a (simple) graph and H is what we will call, for simplicity, an *attachment set*. The attachment 'set' is a cyclic h-tuple of vertices, in which any given vertex is allowed to occur more than once.

Note that in the case of cyclic tuples we do not distinguish between the tuple (v_1, v_2, \ldots, v_h) and its circular shifts $(v_{i+1}, v_{i+2}, \ldots, v_h, v_1, v_2, \ldots, v_i)$ for $1 \le i < h$. In [34], the attachment set was called the peripheral root. Both terms have their disadvantages: the attachment set is not strictly a set, and its vertices may lie in the interior of the graph.

Definition 1. Let G = (V(G), E(G)) be a graph and $H = (v_1, v_2, \dots, v_h)$ be an attachment set, i.e., a cyclic h-tuple with $h \ge 2$ and $v_i \in V(G)$ for $1 \le i \le h$. Let G' be the graph with

$$V(G') = V(G) \sqcup \{x_1, x_2, \dots, x_h\} \sqcup \{y_1, y_2, \dots, y_h\},$$

$$E(G') = E(G) \sqcup \{v_i x_i, x_i y_i : 1 \le i \le h\} \sqcup \{y_i x_{i+1} : 1 \le i < h\} \sqcup \{y_h x_1\}.$$

and let $H' = (y_1, y_2, \dots, y_h)$. The altan of (G, H), denoted $\mathfrak{a}(G, H)$, is the pair (G', H'), where this particular choice of H' will be called the *induced attachment set*.

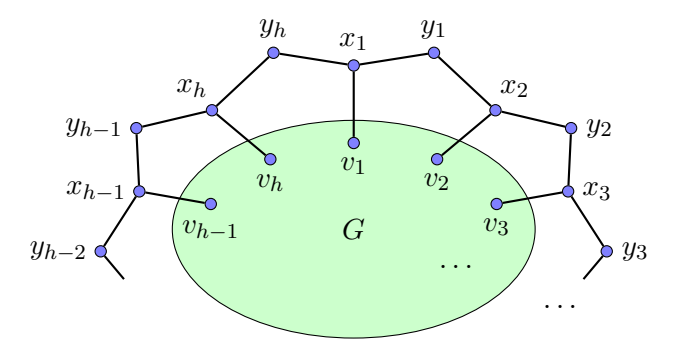


Figure 1: The altan $\mathfrak{a}(G, H)$. Attachment is via the set $\{v_1, \ldots, v_h\}$, possibly with multiple connections to some vertices, and the perimeter is the cycle $\{x_1, y_1, \ldots, x_h, y_h\}$.

For an illustration of the definition see Figure 1. In the above definition, the symbol \sqcup denotes a disjoint union. Observe that |V(G')| = |V(G)| + 2h and |E(G')| = |E(G)| + 3h. The graph G may be disconnected. The graph G' is connected if and only if the attachment set H contains at least one vertex from each connected component of G. Note that the induced attachment set H' is only one possible choice of attachment set for a subsequent altan operation on G'; however, this choice is conveniently used to define an *iterated altan* construction:

$$\mathfrak{a}^{k}(G,H) = \begin{cases} (G,H) & \text{if } k = 0, \\ \mathfrak{a}(G,H) & \text{if } k = 1, \\ \mathfrak{a}(\mathfrak{a}^{k-1}(G,H)) & \text{if } k \geq 2. \end{cases}$$

This recursive definition implicitly defines the sequence of intermediate graphs and their respective attachment sets (see Figure 2). We call $\mathfrak{a}^k(G, H)$ the k-th altan of (G, H).

We recall some basic concepts from spectral graph theory. Let A(G) denote the adjacency matrix of a graph G. Graph G is called singular if A(G) has a non-trivial kernel. The nullity of G, denoted $\eta(G)$, is the algebraic multiplicity of the number 0 in the spectrum of A(G), i.e. $\eta(G) = \dim \ker A(G)$. An eigenvector \mathbf{q} of A(G) can be viewed as a weighting of vertices

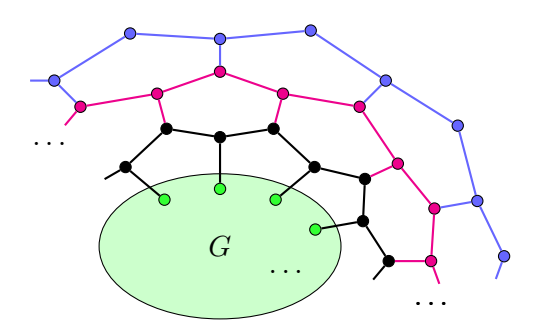


Figure 2: The iterated altan $\mathfrak{a}^3(G, H)$. Colours indicate the new vertices and edges that are added at each stage.

of G, i.e., a mapping $\mathbf{q}: V(G) \to \mathbb{R}$. Let λ be an eigenvalue of A(G), let $v \in V(G)$ and let $N_G(v)$ denote the neighbourhood of v. The equation

$$\lambda \mathbf{q}(v) = \sum_{u \in N_G(v)} \mathbf{q}(u) \tag{1}$$

is sometimes called the local condition (with the pivot v). The notation $u \in N_G(v)$ will be abbreviated $u \sim v$ for convenience. We will be using the local condition for the eigenvalue $\lambda = 0$, in particular.

Application of Hückel theory in organic chemistry is usually limited to systems where the molecular graph is a *chemical graph*, i.e. a graph that is simple, connected and with maximum degree at most three. Altanisation of a chemical graph with an arbitrary attachment set may lead to a non-chemical result, but this can be avoided by choosing a 'natural' attachment set based on the implied hydrogen positions in the chemical formula for the parent chemical graph. One interpretation of this chemically motivated construction is that it represents the formal replacement of all hydrogen atoms of an unsaturated hydrocarbon by vinyl groups, which then cyclise in a particular way [33].

Example 1. Let P_3 be the path on three vertices and let $V(P_3) = \{u_1, u_2, u_3\}$. It is easy to check that $\eta(P_3) = 1$. We will consider the following four attachment sets:

$$H_1 = \{u_1, u_1, u_2, u_3, u_3\}, \quad H_2 = \{u_1, u_3\}, \quad H_3 = \{u_1, u_2, u_3, u_2\}, \quad H_4 = \{u_1, u_1, u_3, u_3\}.$$

It is easy to verify that

$$\eta(\mathfrak{a}(P_3, H_1)) = \eta(\mathfrak{a}(P_3, H_2)) = 1, \qquad \eta(\mathfrak{a}(P_3, H_3)) = 2, \qquad \eta(\mathfrak{a}(P_3, H_4)) = 3.$$

Kernel eigenvectors of the parent graph P_3 and the four altans are shown in Figure 3.

The altan $\mathfrak{a}(P_3, H_3)$ includes a vertex of degree four and is thus not chemical, but it does illustrate the case where $\eta(\mathfrak{a}(P_3, H_3)) = \eta(P_3) + 1$. The present example shows that even a small graph can produce a range of nullities; in fact, it turns out that this example demonstrates all the possibilities, as the theorems below will demonstrate.

2.2 Patches

Most applications of the altan construction in the chemical literature are expansions of a particular kind of polycyclic chemical graph. We call this a *patch*.

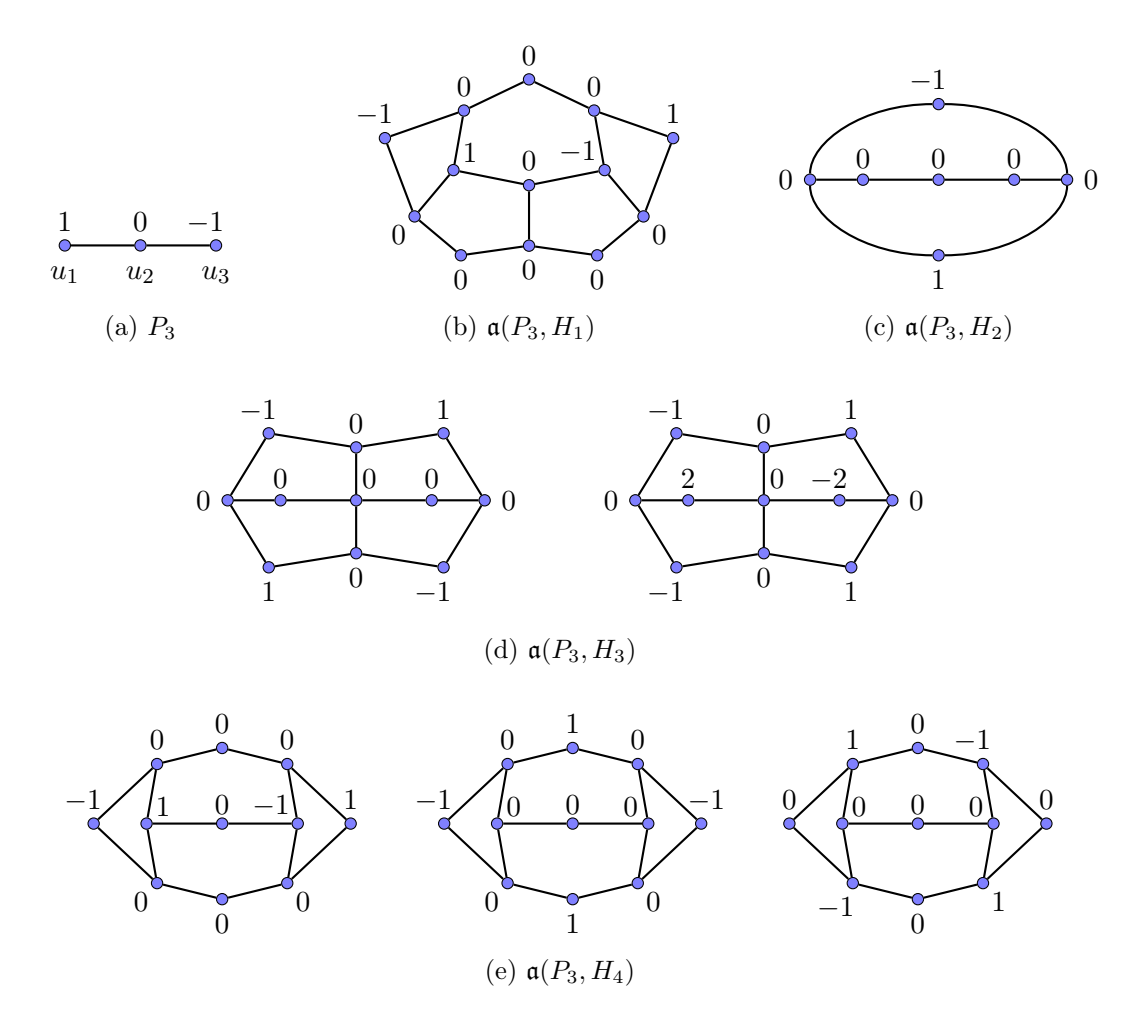


Figure 3: Kernel eigenvectors of (a) the path graph P_3 and (b) – (e) altans for different choices of attachment set. The vectors are chosen to be orthogonal, with integer entries and distinct symmetries in the point group of the altan graph. In (b), the altan has a vertical line of reflection and the kernel eigenvector is (–), i.e. anti-symmetric. In (c) to (e), the altan has horizontal and vertical lines of reflection, and the various kernel eigenvectors have symmetries as follows: (c) (-,+); (d) (-,-) and (+,-); (e) (+,-), (+,+) and (-,-), where the +/- signs indicate symmetry or anti-symmetry with respect to horizontal and vertical lines of reflection, respectively.

Definition 2. A patch Π is a sub-cubic 2-connected plane graph that has every degree-2 vertex incident with the distinguished outer face. The natural attachment set of Π is the htuple H that contains all the degree-2 vertices of Π in the order induced by clockwise traversal of the perimeter (i.e. the outer face). When H is the natural attachment set of a patch Π , we can simplify the notation $\mathfrak{a}(\Pi, H)$ to $\mathfrak{a}(\Pi)$.

Definition 3. A patch that contains only hexagonal interior faces is called a *fusene*. A fusene patch that is a simply connected subgraph of the hexagonal tessellation of the plane is a *benzenoid*. Every benzenoid is a fusene, but not every fusene is a benzenoid.

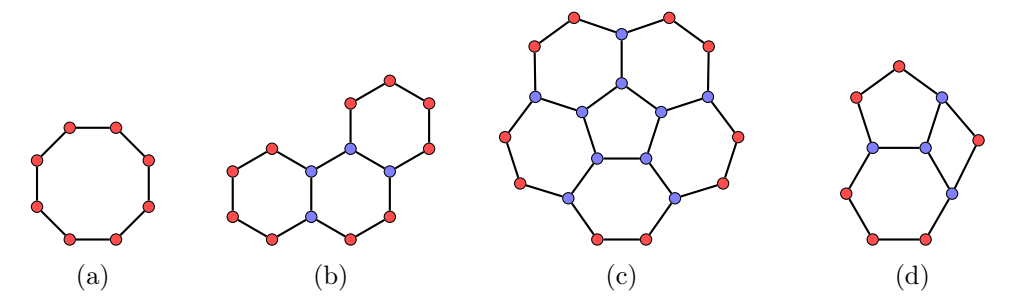


Figure 4: Examples of patches. The vertices of the natural attachment set are coloured red. Patch (b) is a fusene (and a benzenoid). Patches (b) and (c) are fullerene patches in the sense that they can appear as induced subgraphs in fullerenes [46, 47].

Figure 4 contains several examples of patches. A patch is a chemical graph and it corresponds to an unsaturated hydrocarbon of chemical formula C_nH_{3n-2m} where n is the number of vertices and m is the number of edges in the patch. When the altan construction is performed on a patch (which is, by definition, embedded in the plane), the new perimeter cycle can be drawn in the outer face of the patch and connected to the natural attachment set in such a way that no crossings are introduced. The graph obtained is evidently plane. It is easy to see that the altan of a patch is a patch.

Example 2. The molecular graph of pentalene is an example of a small patch, consisting in this case of two fused pentagons. Pentalene has a unique kernel eigenvector/NBMO which is illustrated in Figure 5(a). Altan-pentalene has nullity 2, and a pair of eigenvectors/NBMOs spanning the kernel is shown in Figure 5(b).

Straightforward considerations based on the Euler theorem give relations that constrain the composition of the altan of a patch in terms of the faces that it contains, and of the composition of the cyclic strip of faces that is added to the patch at each stage of altanisation.

Proposition 1. Let Π be a patch. Let f_r denote the number of faces of length r in $\mathfrak{a}(\Pi)$, excluding the infinite (unbounded) face. Then

$$\sum_{r\geq 3} (6-r)f_r = 3f_3 + 2f_4 + f_5 - f_7 - 2f_8 - \dots = 6.$$
 (2)

Let n_k be the number of vertices of degree k in Π and let n_k^b be the number of vertices of degree k on the perimeter of Π . Let \tilde{f}_r denote the number of new faces of length r that are added to

the patch by the altan construction. Then

$$\sum_{r\geq 3} (6-r)\widetilde{f}_r = 3\widetilde{f}_3 + 2\widetilde{f}_4 + \widetilde{f}_5 - \widetilde{f}_7 - 2\widetilde{f}_8 - \dots = n_2 - n_3^b$$
 (3)

with $\widetilde{f}_3 = \widetilde{f}_4 = 0$.

Proof. Let f be the number of faces of $\mathfrak{a}(\Pi)$, excluding the infinite face. Then $f = f_3 + f_4 + f_5 + \cdots = \sum_{r \geq 3} f_r$. Let h be the size of the natural attachment set. Note that $h = n_2^b = n_2$. By applying the Euler formula on the altan $\mathfrak{a}(\Pi)$ we obtain

$$(n_2 + n_3 + 2h) - (n_2 + \frac{3}{2}n_3 + 3h) + (\sum_{r>3} f_r + 1) = 2,$$
(4)

and the Handshaking Lemma for faces gives

$$\sum_{r>3} r f_r + 2h = 2n_2 + 3n_3 + 6h. \tag{5}$$

Combining equations (4) and (5) gives (2).

By applying the Euler formula on the patch Π we obtain

$$(n_2 + n_3) - (n_2 + \frac{3}{2}n_3) + (\sum_{r>3} (f_r - \widetilde{f}_r) + 1) = 2,$$
(6)

while the Handshaking Lemma for faces gives

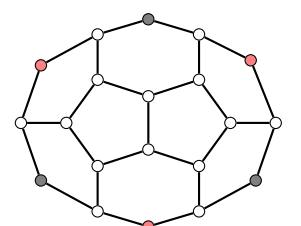
$$\sum_{r\geq 3} r(f_r - \widetilde{f_r}) + (n_3^b + n_2^b) = 2n_2 + 3n_3.$$
 (7)

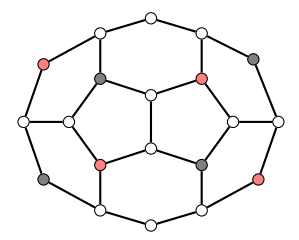
Combining equations (2), (6) and (7) gives (3), and by definition of the altan, it is clear that the length of each new face is at least 5, hence $\tilde{f}_3 = \tilde{f}_4 = 0$.

If $n_3^b=0$ then $\widetilde{f}_5=n_2$ and $\widetilde{f}_7=\widetilde{f}_8=\cdots=0$. Note that in the iterated altan, the boundary code is $(23)^h$ for all altanisations after the first, and $\widetilde{f}_6=h$ while $\widetilde{f}_7=\widetilde{f}_8=1$



(a) The kernel eigenvector of pentalene.





(b) Two orthogonal kernel eigenvectors of altan-pentalene.

Figure 5: The molecular graph of pentalene has nullity 1, whilst the molecular graph of altanpentalene has nullity 2. Eigenvector entries are colour-coded: white corresponds to value 0, black to 1 and red to -1 in the unnormalised vector. In the normalised vectors, entries are multiplied by $\sqrt{1/4}$, $\sqrt{1/6}$ and $\sqrt{1/8}$, respectively. $\widetilde{f}_9 = \cdots = 0$. Iteration will lead to a graphitic tube corresponding to a capped nanotube (a nanocone with 6 disclinations in the nomenclature of Klein and Balaban [48]).

Reasoning of this type is often used to describe the composition of various types of generalised patch [32,49]. In [32] it is used to specify the composition of the altans of benzenoids. In the familiar geographical analogy where the perimeter of a benzenoid is likened to the coastline of an island continent, regions of increasing concavity are described as fissures, bays, coves and fjords [50], corresponding respectively to degree sequences on the boundary of 232, 2332, 23332, and 233332. The counts of the four types of feature are denoted b_1 , b_2 , b_3 , and b_4 , respectively. The bay number of the benzenoid is then $b = b_2 + 2b_3 + 3b_4$, and the number of adjacencies of type 22 on the perimeter of the benzenoid is $n_{22} = 6 + b$ [50], which is also the number of pentagons added to the benzenoid by altanisation. Each fissure, bay, cove or fjord adds respectively a hexagon, heptagon, octagon or nonagon in the altan [32]. Hence, when G is a benzenoid, in our notation we have

$$\widetilde{f}_5 - \widetilde{f}_7 - 2\widetilde{f}_8 - 3\widetilde{f}_9 = 6, \tag{8}$$

which is the special case of (3) for a benzenoid parent. Notice also that *convex* benzenoids [51] have b = 0, so that the strip of faces added by the altan operation to a convex benzenoid consists of 6 pentagons and b_1 hexagons.

Simple counting considerations can also be used to derive a useful relation between nullity and size of the attachment set in the case where the patch is bipartite:

Theorem 2. Let Π be a bipartite patch and let H be the natural attachment set. Then

$$\eta(\Pi) \equiv |H| \pmod{2}.$$

Proof. Let $V(\Pi)$ and $E(\Pi)$ be the vertex and edge sets of the patch Π , respectively. Let n_2 and n_3 denote the numbers of degree-2 and degree-3 vertices of the patch. Moreover, let n_3^i and n_3^b denote the numbers of internal and boundary degree-3 vertices of the patch, respectively. Note that $n_3 = n_3^i + n_3^b$ and $n = |V(\Pi)| = n_2 + n_3$. Furthermore, let p denote the length of the perimeter. Note that $p = n_2 + n_3^b$. Observe that $h = |H| = n_2$.

Since Π is a bipartite graph, all its cycles are of even length and therefore p is even. From $p=n_2+n_3^b\equiv 0\pmod 2$ it follows that $n_2\equiv n_3^b\pmod 2$. From $n=n_2+n_3^b+n_3^i$ it follows that $n\equiv n_3^i\pmod 2$. By the Handshaking Lemma, $2|E(\Pi)|=3n_3+2n_2$ and therefore $n_3\equiv 0\pmod 2$. Hence, $n_3^b\equiv n_3^i\pmod 2$. By the Pairing Theorem, $n\equiv \eta(\Pi)\pmod 2$. Summarising the above observations we obtain

$$h \equiv n_3^i \equiv n_3^b \equiv n \equiv \eta(\Pi) \pmod{2}.$$

Corollary 3. Let \mathcal{B} be a benzenoid on n vertices, let $\eta = \eta(\mathcal{B})$ be the nullity of \mathcal{B} and let h be the size of the natural attachment set. Then

$$h \equiv n \equiv \eta \pmod{2}$$
.

In the proof of Theorem 2 we have seen that $n_2 \equiv n_3^b \pmod{2}$ for a bipartite patch. This implies that the altan of a bipartite patch has a constraint on the numbers of faces of odd lengths. In this case, the RHS of Equation (3) is even and $\tilde{f}_5 - \tilde{f}_7 - 3\tilde{f}_9 - 5\tilde{f}_{11} - \cdots \equiv 0 \pmod{2}$.

Although we have concentrated here on altanisation of patched as models for simply connected polycyclic aromatic hydrocarbon (PAH) nanostructures, the chemical literature also includes examples of altans of structures with holes, such as kekulene [52], where altanisation proceeds on the outer perimeter only. Altans (inner and outer) of general coronoid structures such as kekulene have been considered in [35] under a comprehensive scheme for altanisation of perforated patches.

3 Main results: Theorems for nullities of altans

We can now state the main results of our mathematical investigation of the nullity of altans.

Definition 4. Let (G', H') and vertex labeling be as in Definition 1 (see also Figure 1). The vector \mathbf{s} , defined as

$$\mathbf{s}(u) = \begin{cases} 1 & \text{if } u = y_i \text{ and } i \text{ even,} \\ -1 & \text{if } u = y_i \text{ and } i \text{ odd,} \\ 0 & \text{otherwise,} \end{cases}$$
 (9)

will be called the *special vector* of $\mathfrak{a}(G,H)$, or sometimes, for short, the special one.

An example of this vector has already been encountered in Example 2 (see the left panel of Figure 5(b)).

Lemma 4. Let (G', H') be as in Definition 4. If h = |H| is even, then the special vector \mathbf{s} is a kernel eigenvector of $\mathfrak{a}(G, H)$.

Proof. Apply the local condition (1) with $\lambda = 0$. If h is even then $\{\mathbf{s}(u) : u \in N(x_i)\} = \{-1, 0, 1\}$ for all $1 \le i \le h$. For all other vertices $w \ne x_i$ we have $\{\mathbf{s}(u) : u \in N(w)\} = \{0\}$. \square

The following theorem was already proved by Gutman in [33] using the Sachs Theorem. Here, we give an elementary proof.

Theorem 5 (Gutman [33]). Let G be a graph and let H be an even attachment set. Then $\eta(\mathfrak{a}(G,H)) \geq 1$.

Proof. Follows directly from Lemma 4.

Theorem 6. Let G be a graph and let H be an attachment set. Then

$$\eta(\mathfrak{a}(G,H)) \ge \eta(G). \tag{10}$$

Proof. Let $(G', H') = \mathfrak{a}(G, H)$ and let G' be labelled as in Definition 1. Let $\mathbf{q} \in \ker(G)$. We will extend the vector \mathbf{q} to $\widetilde{\mathbf{q}} \in \ker(G')$. Let $\widetilde{\mathbf{q}}(u) = \mathbf{q}(u)$ for $u \in V(G)$ and let $\widetilde{\mathbf{q}}(x_i) = 0$ for all $1 \leq i \leq h$. Note that all vertices $v \in V(G)$ and $v \in V(G)$ are $v \in V(G)$.

Now, let $\widetilde{\mathbf{q}}(y_h) = t \in \mathbb{R}$. By pivoting at vertices x_1, x_2, \dots, x_{h-1} , respectively, we obtain

$$\widetilde{\mathbf{q}}(y_1) = -t - \widetilde{\mathbf{q}}(v_1)$$

$$\widetilde{\mathbf{q}}(y_2) = t + \widetilde{\mathbf{q}}(v_1) - \widetilde{\mathbf{q}}(v_2)$$

$$\widetilde{\mathbf{q}}(y_3) = -t - \widetilde{\mathbf{q}}(v_1) + \widetilde{\mathbf{q}}(v_2) - \widetilde{\mathbf{q}}(v_3)$$

$$\cdots$$

$$\widetilde{\mathbf{q}}(y_{h-1}) = \begin{cases} -t - \widetilde{\mathbf{q}}(v_1) + \widetilde{\mathbf{q}}(v_2) - \widetilde{\mathbf{q}}(v_3) + \cdots - \widetilde{\mathbf{q}}(v_{h-1}) & \text{if } h \text{ even,} \\ t + \widetilde{\mathbf{q}}(v_1) - \widetilde{\mathbf{q}}(v_2) + \widetilde{\mathbf{q}}(v_3) - \cdots - \widetilde{\mathbf{q}}(v_{h-1}) & \text{if } h \text{ odd.} \end{cases}$$

Let us define

$$C(\mathbf{q}) = \sum_{i=1}^{h} (-1)^{i} \mathbf{q}(v_i). \tag{11}$$

It is easy to see that C is a linear functional. By pivoting at vertex x_h , we get the following condition

$$\begin{cases} \mathcal{C}(\mathbf{q}) = 0 & \text{if } h \text{ even,} \\ t = \frac{1}{2}\mathcal{C}(\mathbf{q}) & \text{if } h \text{ odd.} \end{cases}$$
 (12)

Now, let $\eta = \eta(G)$ and let $\{\mathbf{q}^{(1)}, \mathbf{q}^{(2)}, \dots, \mathbf{q}^{(\eta)}\}$ be a basis of $\ker(G)$. In other words, $\ker(G) = \operatorname{span}\{\mathbf{q}^{(1)}, \mathbf{q}^{(2)}, \dots, \mathbf{q}^{(\eta)}\}$ and vectors $\mathbf{q}^{(1)}, \mathbf{q}^{(2)}, \dots, \mathbf{q}^{(\eta)}$ are linearly independent.

First, suppose that h is odd. From (12) it follows that each vector $\mathbf{q}^{(k)}$ can be extended to $\widetilde{\mathbf{q}}^{(k)}$ by setting $t = \frac{1}{2}\mathcal{C}(\mathbf{q}^{(k)})$, as described above. By construction, $\{\widetilde{\mathbf{q}}^{(1)}, \widetilde{\mathbf{q}}^{(2)}, \dots, \widetilde{\mathbf{q}}^{(\eta)}\} \subseteq \ker(G')$. It is easy to see that these vectors are linearly independent. Therefore, $\eta(G') \geq \eta(G)$.

Suppose instead that h is even. A kernel eigenvector \mathbf{q} will be called *extendable* if $\mathcal{C}(\mathbf{q}) = 0$, i.e., if it satisfies condition (12). We consider two cases:

- (i) Suppose that vectors $\mathbf{q}^{(1)}, \mathbf{q}^{(2)}, \dots, \mathbf{q}^{(\eta)}$ are all extendable. Then their extensions $\widetilde{\mathbf{q}}^{(1)}, \widetilde{\mathbf{q}}^{(2)}, \dots, \widetilde{\mathbf{q}}^{(\eta)}$ are obtained as described above by choosing, say, t = 0. It is easy to see that the vectors $\widetilde{\mathbf{q}}^{(1)}, \widetilde{\mathbf{q}}^{(2)}, \dots, \widetilde{\mathbf{q}}^{(\eta)}$ are linearly independent. Moreover, the special vector \mathbf{s} is yet another kernel eigenvector. It is easy to check that \mathbf{s} is linearly independent of all vectors $\widetilde{\mathbf{q}}^{(1)}, \widetilde{\mathbf{q}}^{(2)}, \dots, \widetilde{\mathbf{q}}^{(\eta)}$ (by inspecting the entry y_h). Hence, in this case we get $\eta(G') \geq \eta(G) + 1$.
- (ii) Suppose that at least one of the vectors $\mathbf{q}^{(1)}, \mathbf{q}^{(2)}, \dots, \mathbf{q}^{(\eta)}$ is not extendable. Without loss of generality, assume that $\mathbf{q}^{(1)}$ is not extendable. In other words, $\mathcal{C}(\mathbf{q}^{(1)}) \neq 0$. We will replace the basis $\{\mathbf{q}^{(1)}, \mathbf{q}^{(2)}, \dots, \mathbf{q}^{(\eta)}\}$ with an alternative basis

$$\{\mathbf{q}^{(1)}, \mathbf{q}^{(2)} + \lambda_2 \mathbf{q}^{(1)}, \mathbf{q}^{(3)} + \lambda_3 \mathbf{q}^{(1)}, \dots, \mathbf{q}^{(\eta)} + \lambda_n \mathbf{q}^{(1)}\},$$

where scalars λ_k are chosen so that $\mathcal{C}(\mathbf{q}^{(k)} + \lambda_k \mathbf{q}^{(1)}) = 0$. Namely, $\lambda_k = -\mathcal{C}(\mathbf{q}^{(k)})/\mathcal{C}(\mathbf{q}^{(1)})$. Let $\widetilde{\mathbf{q}}^{(2)}, \dots, \widetilde{\mathbf{q}}^{(\eta)}$ be extensions of $\mathbf{q}^{(2)} + \lambda_2 \mathbf{q}^{(1)}, \dots, \mathbf{q}^{(\eta)} + \lambda_\eta \mathbf{q}^{(1)}$, respectively. It is easy to see that the vectors $\widetilde{\mathbf{q}}^{(2)}, \dots, \widetilde{\mathbf{q}}^{(\eta)}$ are linearly independent. Moreover, the special vector \mathbf{s} is independent of them. Again, we get $\eta(G') \geq \eta(G)$, as the special one compensates for the loss of $\mathbf{q}^{(1)}$.

Note that the kernel eigenvector of pentalene (see Figure 5(a)) is extendable, and altanpentalene is an example of case (i) in the proof above.

Theorem 7. Let G be a graph and H an attachment set. Then

$$\eta(\mathfrak{a}(G,H)) \le \begin{cases} \eta(G) + 2 & \text{if } h = |H| \text{ even,} \\ \eta(G) & \text{if } h = |H| \text{ odd.} \end{cases}$$
(13)

To prepare for the proof of the above theorem, we state several technical lemmas.

Lemma 8. Let (G', H') be as in Definition 1. Let $\widetilde{\mathbf{q}} \in \ker(G')$. If h is odd then $\widetilde{\mathbf{q}}(x_i) = 0$ for all $1 \leq i \leq h$.

Proof. Let $\widetilde{\mathbf{q}}(x_1) = t \in \mathbb{R}$. By pivoting at vertices y_1, y_2, \dots, y_{h-1} , respectively, we obtain

$$\widetilde{\mathbf{q}}(x_1) = \widetilde{\mathbf{q}}(x_3) = \widetilde{\mathbf{q}}(x_5) = \dots = \widetilde{\mathbf{q}}(x_h) = t,$$

 $\widetilde{\mathbf{q}}(x_2) = \widetilde{\mathbf{q}}(x_4) = \widetilde{\mathbf{q}}(x_4) = \dots = \widetilde{\mathbf{q}}(x_{h-1}) = -t.$

By pivoting at vertex y_h we obtain t = 0.

Lemma 9. Let (G', H') be as in Definition 1. Let $\widetilde{\mathbf{q}} \in \ker(G')$ such that $\widetilde{\mathbf{q}}(u) = 0$ for all $u \in V(G)$ and $\widetilde{\mathbf{q}}(x_i) = 0$ for all $1 \le i \le h$. If h is odd then $\widetilde{\mathbf{q}}(y_i) = 0$ for all $1 \le i \le h$.

Proof. Let $\widetilde{\mathbf{q}}(y_1) = t \in \mathbb{R}$. By pivoting at vertices x_2, x_3, \ldots, x_h , respectively, we obtain

$$\widetilde{\mathbf{q}}(y_1) = \widetilde{\mathbf{q}}(y_3) = \widetilde{\mathbf{q}}(y_5) = \dots = \widetilde{\mathbf{q}}(y_h) = t,$$

 $\widetilde{\mathbf{q}}(y_2) = \widetilde{\mathbf{q}}(y_4) = \widetilde{\mathbf{q}}(y_4) = \dots = \widetilde{\mathbf{q}}(y_{h-1}) = -t.$

By pivoting at vertex x_1 we obtain t = 0.

Lemma 10. Let (G', H') be as in Definition 1. Let $\widetilde{\mathbf{q}} \in \ker(G')$. If h is even then $\widetilde{\mathbf{q}}(x_i) = \widetilde{\mathbf{q}}(x_1)$ for all odd i and $\widetilde{\mathbf{q}}(x_i) = -\widetilde{\mathbf{q}}(x_1)$ for all even i.

Proof. The proof is similar to that of Lemma 8 and is left to the reader. \Box

Lemma 11. Let (G', H') be as in Definition 1. Let $\widetilde{\mathbf{q}} \in \ker(G')$ such that $\widetilde{\mathbf{q}}(u) = 0$ for all $u \in V(G)$ and $\widetilde{\mathbf{q}}(x_i) = 0$ for all $1 \le i \le h$. If h is even then $\widetilde{\mathbf{q}}(y_i) = \widetilde{\mathbf{q}}(y_1)$ for all odd i and $\widetilde{\mathbf{q}}(y_i) = -\widetilde{\mathbf{q}}(y_1)$ for all even i.

Proof. The proof is similar to that of Lemma 9 and is left to the reader. \Box

Now we can give the proof of Theorem 7.

Proof of Theorem 7. Let $(G', H') = \mathfrak{a}(G, H)$ and let G' be labelled as in Definition 1.

First, suppose that h is odd. Let $\xi = \eta(G')$ and let $\{\widetilde{\mathbf{q}}^{(1)}, \widetilde{\mathbf{q}}^{(2)}, \dots, \widetilde{\mathbf{q}}^{(\xi)}\}\$ be a basis for $\ker(G')$. A kernel eigenvector $\widetilde{\mathbf{q}}$ of G' will be called *contractible* if $\widetilde{\mathbf{q}}(x_i) = 0$ for all $1 \le i \le h$. The *contraction* of $\widetilde{\mathbf{q}}$ is the vector \mathbf{q} of G defined by $\mathbf{q}(u) = \widetilde{\mathbf{q}}(u)$ for $u \in V(G)$. Note that $\mathbf{q} \in \ker(G)$ if $\widetilde{\mathbf{q}}$ is contractible.

By Lemma 8, the vectors $\widetilde{\mathbf{q}}^{(1)}, \widetilde{\mathbf{q}}^{(2)}, \dots, \widetilde{\mathbf{q}}^{(\xi)}$ are contractible. Let $\mathbf{q}^{(1)}, \mathbf{q}^{(2)}, \dots, \mathbf{q}^{(\xi)}$ be contractions of $\widetilde{\mathbf{q}}^{(1)}, \widetilde{\mathbf{q}}^{(2)}, \dots, \widetilde{\mathbf{q}}^{(\xi)}$, respectively. We will prove that $\mathbf{q}^{(1)}, \mathbf{q}^{(2)}, \dots, \mathbf{q}^{(\xi)}$ are linearly independent. For contradiction, suppose that they are not linearly independent. Then there exist scalars $\mu_1, \mu_2, \dots, \mu_{\xi}$ (at least one of which is non-zero) such that

$$\mu_1 \mathbf{q}^{(1)} + \mu_2 \mathbf{q}^{(2)} + \dots + \mu_{\xi} \mathbf{q}^{(\xi)} = \mathbf{0}.$$
 (14)

Let us define

$$\mathbf{Q} := \mu_1 \widetilde{\mathbf{q}}^{(1)} + \mu_2 \widetilde{\mathbf{q}}^{(2)} + \dots + \mu_{\xi} \widetilde{\mathbf{q}}^{(\xi)}.$$

Observe that $\mathbf{Q}(u) = (\mu_1 \mathbf{q}^{(1)} + \mu_2 \mathbf{q}^{(2)} + \dots + \mu_{\xi} \mathbf{q}^{(\xi)})(u)$ for all $u \in V(G)$. From (14) it follows that $\mathbf{Q}(u) = 0$ for all $u \in V(G)$. By Lemma 9, $\mathbf{Q} = \mathbf{0}$. This contradicts the fact that $\{\widetilde{\mathbf{q}}^{(1)}, \widetilde{\mathbf{q}}^{(2)}, \dots, \widetilde{\mathbf{q}}^{(\xi)}\}$ is a basis, so $\mathbf{q}^{(1)}, \mathbf{q}^{(2)}, \dots, \mathbf{q}^{(\xi)}$ are linearly independent and hence $\eta(G) \geq \eta(G')$.

Suppose instead that h is even. Let $\xi = \eta(G')$. By Lemma 4, we have $\mathbf{s} \in \ker(G')$. We can choose a basis that contains the special one, so let $\{\mathbf{s}, \widetilde{\mathbf{q}}^{(2)}, \dots, \widetilde{\mathbf{q}}^{(\xi)}\}$ be a basis for $\ker(G')$.

Note that **s** is contractible, but its contraction is the trivial vector **0**. Let us assume to begin with that at least one of the vectors $\widetilde{\mathbf{q}}^{(2)}, \ldots, \widetilde{\mathbf{q}}^{(\xi)}$ is *not* contractible; without loss of generality, we take $\widetilde{\mathbf{q}}^{(2)}$ to be non-contractible. The vectors $\widetilde{\mathbf{q}}^{(3)}, \ldots, \widetilde{\mathbf{q}}^{(\xi)}$ can be replaced by

$$\widetilde{\mathbf{q}}^{(3)} + \lambda_3 \widetilde{\mathbf{q}}^{(2)}, \widetilde{\mathbf{q}}^{(4)} + \lambda_4 \widetilde{\mathbf{q}}^{(2)}, \dots, \widetilde{\mathbf{q}}^{(\xi)} + \lambda_{\xi} \widetilde{\mathbf{q}}^{(2)},$$
 (15)

where scalars $\lambda_3, \lambda_4, \ldots, \lambda_{\xi}$ can be chosen in such a way that the vectors specified in (15) are all contractible; namely, by setting $\lambda_k = -\widetilde{\mathbf{q}}^{(k)}(x_1)/\widetilde{\mathbf{q}}^{(2)}(x_1)$. (Note that $\widetilde{\mathbf{q}}^{(2)}(x_1)$ is non-zero, because $\widetilde{\mathbf{q}}^{(2)}$ would otherwise be contractible by Lemma 10.) The vector $\widetilde{\mathbf{q}}^{(k)} + \lambda_k \widetilde{\mathbf{q}}^{(2)}$ is then contractible by Lemma 10. Therefore, we can assume that all basis vectors, except possibly the vector $\widetilde{\mathbf{q}}^{(2)}$, are contractible.

First, assume that $\widetilde{\mathbf{q}}^{(2)}$ is non-contractible. Let $\mathbf{q}^{(3)}, \mathbf{q}^{(4)}, \dots, \mathbf{q}^{(\xi)}$ be contractions of vectors $\widetilde{\mathbf{q}}^{(3)}, \widetilde{\mathbf{q}}^{(4)}, \dots, \widetilde{\mathbf{q}}^{(\xi)}$, respectively. We will prove that $\mathbf{q}^{(3)}, \mathbf{q}^{(4)}, \dots, \mathbf{q}^{(\xi)}$ are linearly independent. For contradiction, suppose that they are not linearly independent. Then there exist scalars $\mu_3, \mu_4, \dots, \mu_{\xi}$ (at least one of which is non-zero) such that

$$\mu_3 \mathbf{q}^{(3)} + \mu_4 \mathbf{q}^{(4)} + \dots + \mu_{\xi} \mathbf{q}^{(\xi)} = \mathbf{0}.$$
 (16)

Let us define

$$\mathbf{Q} := \mu_3 \widetilde{\mathbf{q}}^{(3)} + \mu_4 \widetilde{\mathbf{q}}^{(4)} + \dots + \mu_{\varepsilon} \widetilde{\mathbf{q}}^{(\xi)}.$$

Observe that $\mathbf{Q}(u) = (\mu_3 \mathbf{q}^{(3)} + \mu_4 \mathbf{q}^{(4)} + \dots + \mu_{\xi} \mathbf{q}^{(\xi)})(u)$ for all $u \in V(G)$. From (16) it follows that $\mathbf{Q}(u) = 0$ for all $u \in V(G)$. As $\widetilde{\mathbf{q}}^{(3)}, \widetilde{\mathbf{q}}^{(4)}, \dots, \widetilde{\mathbf{q}}^{(\xi)}$ are contractible, it also follows that $\mathbf{Q}(x_i) = 0$ for all $1 \leq i \leq h$. By Lemma 11, it follows that $\mathbf{Q} = \sigma \mathbf{s}$ for some scalar σ . Therefore,

$$\mu_3 \widetilde{\mathbf{q}}^{(3)} + \mu_4 \widetilde{\mathbf{q}}^{(4)} + \dots + \mu_{\varepsilon} \widetilde{\mathbf{q}}^{(\xi)} - \sigma \mathbf{s} = \mathbf{0}.$$

This contradicts the fact that $\{\mathbf{s}, \widetilde{\mathbf{q}}^{(2)}, \dots, \widetilde{\mathbf{q}}^{(\xi)}\}$ is a basis, so $\mathbf{q}^{(3)}, \mathbf{q}^{(4)}, \dots, \mathbf{q}^{(\xi)}$ are linearly independent and hence $\eta(G) \geq \eta(G') - 2$.

The case where $\widetilde{\mathbf{q}}^{(2)}$ is contractible is analogous, except that we obtain $\eta(G) \geq \eta(G') - 1$. Either way, $\eta(G') \leq \eta(G) + 2$, as desired.

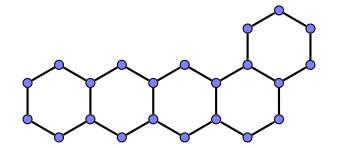
Combining the bounds in Theorems 6 and 7, we obtain our main result for the possible values of the nullity of an altan:

Corollary 12. Let G be a graph and H an attachment set.

- (i) If h = |H| is even then $\eta(G) \le \eta(\mathfrak{a}(G, H)) \le \eta(G) + 2$.
- (ii) If h = |H| is odd then $\eta(\mathfrak{a}(G, H)) = \eta(G)$.

Cases where $\eta(\mathfrak{a}(G,H)) = \eta(G)$ or $\eta(\mathfrak{a}(G,H)) = \eta(G) + 1$ are well known, but, apparently, the case $\eta(\mathfrak{a}(G,H)) = \eta(G) + 2$ had not been noticed before. Exhaustive search shows that the smallest benzenoid that gains two NBMOs on altanisation is a 5-hexagon molecule (benzo[a]tetracene, a.k.a. benzo[a]naphthacene), as shown in Figure 6/Example 3.

Example 3. Figure 6(a) shows the molecular graph of benzo[a]tetracene. As a catafused benzenoid, this molecule has no NBMOs (nullity equals 0). Surprisingly, the molecular graph of its altan, on the other hand, has nullity 2. Figures 6(b) and 6(c) show a pair of independent eigenvectors $\mathbf{q}^{(1)}$ and $\mathbf{q}^{(2)}$ spanning the nullspace. Note that the vector $\mathbf{q}^{(1)}$ is, in fact, the special one, which arises whenever the attachment set is even. Orthonormal molecular orbitals can be found by taking combinations $(1/\sqrt{14})\mathbf{q}^{(1)}$ and $(1/\sqrt{162526})(9\mathbf{q}^{(1)}-14\mathbf{q}^{(2)})$. This is the smallest benzenoid for which the excess nullity of the altan is 2.



(a) Benzo[a]tetracene (a.k.a. benzo[a]naphthacene)

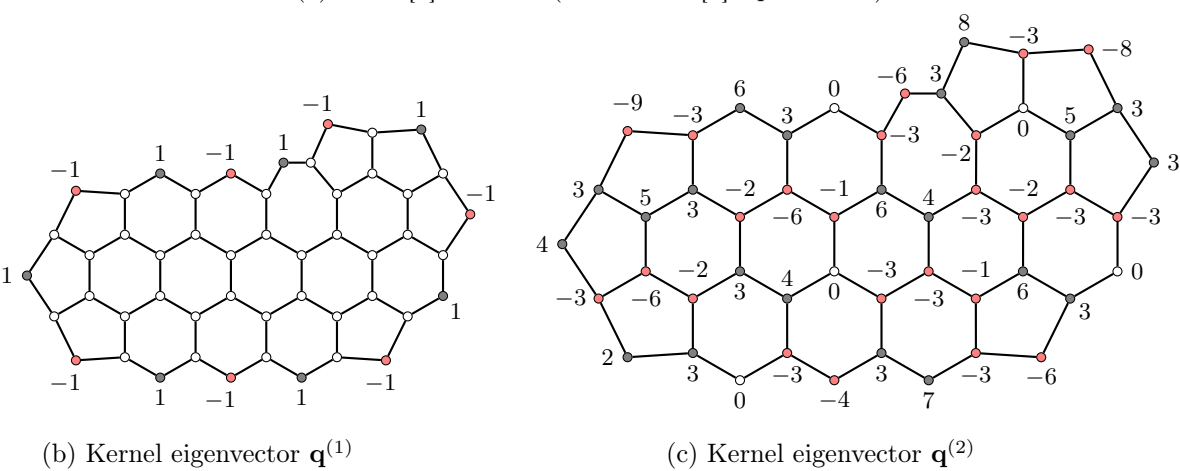


Figure 6: The molecular graph of benzo [a] tetracene and two independent kernel eigenvectors of the altan. In (b) and (c) all vertices represented by white-filled circles carry entry 0.

So far, the complete list of the possible cases for the difference in nullity between a parent graph and its altan was derived from general considerations of linear algebra concerning the possibilities for extension of kernel vectors from parent to altan, and contraction from altan to parent. These considerations can also be used to derive an interesting result for this difference in the case where the parent graph is itself an altan. Again, a preliminary technical lemma is needed.

Lemma 13. Let (G', H') be as in Definition 1. Let $(G'', H'') = \mathfrak{a}(G', H')$ and let vertices of the perimeter of G'' be labeled x_1', x_2', \ldots, x_h' and y_1', y_2', \ldots, y_h' so that $N(x_1') = \{y_h', y_1, y_1'\}$, $N(x_2') = \{y_1', y_2, y_2'\}$, $N(x_3') = \{y_2', y_3, y_3'\}$ and so on (see Figure 7). Let $\mathbf{q} \in \ker(G'')$ and let $\mathcal{D}(\mathbf{q}) = \sum_{i=1}^h (-1)^i \mathbf{q}(y_i)$.

- (i) If h is even then $\mathbf{q}(x_i') = 0$ for all $1 \le i \le h$.
- (ii) If h is even then $\mathcal{D}(\mathbf{q}) = 0$.

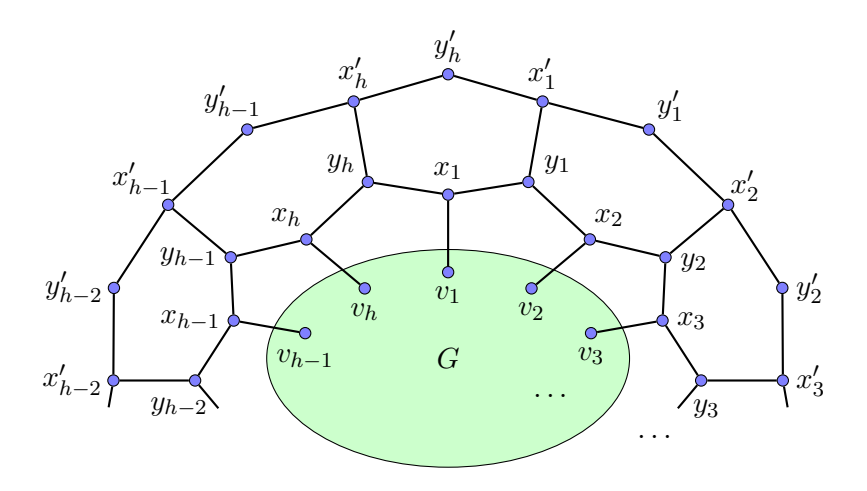


Figure 7: The double altan $(G'', H'') = \mathfrak{a}(G', H') = \mathfrak{a}^2(G, H)$ as described in Lemma 13.

Proof. (i): By Lemma 10, we can write $\mathbf{q}(x_i') = a$ for all even i and $\mathbf{q}(x_i') = -a$ for all odd i. By pivoting at vertices y_1, y_2, \ldots, y_h we get the following conditions:

$$x_{1} + x_{2} = a$$

$$x_{2} + x_{3} = -a$$

$$x_{3} + x_{4} = a$$

$$\cdots$$

$$x_{h-1} + x_{h} = a$$

$$x_{1} + x_{h} = -a$$

$$(17)$$

By summing all rows of (17) we get $\sum_{i=1}^{h} x_i = 0$. By summing all odd rows of (17), we get $\sum_{i=1}^{h} x_i = \frac{h}{2}a$. Hence, a = 0.

(ii): It is easy to see that \mathcal{D} is a linear functional. Now, let $\mathbf{q}(y_h') = t \in \mathbb{R}$. By pivoting at vertices $x_1', x_2', \dots, x_{h-1}'$ we obtain

$$\mathbf{q}(y_1') = -t - \mathbf{q}(y_1)$$

$$\mathbf{q}(y_2') = t + \mathbf{q}(y_1) - \mathbf{q}(y_2)$$

$$\mathbf{q}(y_3') = -t - \mathbf{q}(y_1) + \mathbf{q}(y_2) - \mathbf{q}(y_3)$$

$$\dots$$

$$\mathbf{q}(y_{h-1}') = -t - \mathbf{q}(y_1) + \mathbf{q}(y_2) - \mathbf{q}(y_3) + \dots - \mathbf{q}(y_{h-1}).$$

Finally, by pivoting at vertex x_h' we obtain $\mathbf{q}(y_{h-1}') + t + \mathbf{q}(y_h) = \mathcal{D}(\mathbf{q}) = 0$, as desired. \square

Theorem 14. Let G be a graph and H an attachment set. Then

$$\eta(\mathfrak{a}(G,H)) = \eta(\mathfrak{a}^2(G,H)). \tag{18}$$

Proof. If h = |H| is odd then the statement of the theorem follows from Corollary 12(ii).

Suppose that h = |H| is even. Let $\xi = \eta(G'')$. Let $\tilde{\mathbf{s}} \in \ker(G'')$ denote the special vector of G'' and let $\mathbf{s} \in \ker(G')$ denote the special vector of G'. (The vector \mathbf{s} has non-zero entries on vertices y_i only, whilst the vector $\tilde{\mathbf{s}}$ has non-zero entries on vertices y_i' only.) Vectors \mathbf{s} and $\tilde{\mathbf{s}}$ both exist by Lemma 4. We can choose a basis for G'' that contains the special one, so let $\{\tilde{\mathbf{s}}, \tilde{\mathbf{q}}^{(2)}, \dots, \tilde{\mathbf{q}}^{(\xi)}\}$ be a basis for $\ker(G'')$.

By Lemma 13(i), the vectors $\widetilde{\mathbf{q}}^{(2)}$, $\widetilde{\mathbf{q}}^{(3)}$,..., $\widetilde{\mathbf{q}}^{(\xi)}$ are contractible. Let $\mathbf{q}^{(2)}$, $\mathbf{q}^{(3)}$,..., $\mathbf{q}^{(\xi)}$ be contractions of $\widetilde{\mathbf{q}}^{(2)}$, $\widetilde{\mathbf{q}}^{(3)}$,..., $\widetilde{\mathbf{q}}^{(\xi)}$, respectively. Note that $\mathbf{q}^{(2)}$, $\mathbf{q}^{(3)}$,..., $\mathbf{q}^{(\xi)}$ $\in \ker(G')$.

Since \mathcal{D} (defined in Lemma 13 for vectors $\widetilde{\mathbf{q}} \in \ker(G'')$) involves only the entries y_1, y_2, \ldots, y_h , it remains well defined for vectors $\mathbf{q} \in \ker(G')$. Observe that $\mathcal{D}(\mathbf{q}) = \mathcal{D}(\widetilde{\mathbf{q}})$ if \mathbf{q} is a contraction of $\widetilde{\mathbf{q}}$. The vector \mathbf{s} is linearly independent of $\mathbf{q}^{(2)}, \mathbf{q}^{(3)}, \ldots, \mathbf{q}^{(\xi)}$, since $\mathcal{D}(\mathbf{q}^{(i)}) = 0$ for all $2 \le i \le \xi$ by Lemma 13(ii) and $\mathcal{D}(\mathbf{s}) = h$.

It remains to be proved that the vectors $\mathbf{q}^{(2)}, \mathbf{q}^{(3)}, \dots, \mathbf{q}^{(\xi)}$ are linearly independent of each other. For contradiction, suppose that they are not linearly independent. Then there exist scalars $\mu_2, \mu_3, \dots, \mu_{\xi}$ (at least one of which is non-zero) such that

$$\mu_2 \mathbf{q}^{(2)} + \mu_3 \mathbf{q}^{(3)} + \dots + \mu_{\varepsilon} \mathbf{q}^{(\xi)} = \mathbf{0}.$$
 (19)

Now define

$$\mathbf{Q} := \mu_2 \widetilde{\mathbf{q}}^{(2)} + \mu_3 \widetilde{\mathbf{q}}^{(3)} + \dots + \mu_{\xi} \widetilde{\mathbf{q}}^{(\xi)}.$$

Observe that $\mathbf{Q}(u) = (\mu_2 \mathbf{q}^{(2)} + \mu_3 \mathbf{q}^{(3)} + \cdots + \mu_{\xi} \mathbf{q}^{(\xi)})(u)$ for all $u \in V(G')$. From (19) it follows that $\mathbf{Q}(u) = 0$ for all $u \in V(G')$. From Lemma 13(i) it follows that $\mathbf{Q}(x_i') = 0$ for all $1 \le i \le h$. By Lemma 11, it follows that $\mathbf{Q} = \sigma \widetilde{\mathbf{s}}$ for some scalar σ . Therefore,

$$\mu_2 \widetilde{\mathbf{q}}^{(2)} + \mu_3 \widetilde{\mathbf{q}}^{(3)} + \dots + \mu_{\xi} \widetilde{\mathbf{q}}^{(\xi)} - \sigma \widetilde{\mathbf{s}} = \mathbf{0}.$$

This contradicts the fact that $\{\widetilde{\mathbf{s}}, \widetilde{\mathbf{q}}^{(2)}, \dots, \widetilde{\mathbf{q}}^{(\xi)}\}$ is a basis for $\ker(G'')$.

To summarise, vectors $\mathbf{s}, \mathbf{q}^{(2)}, \mathbf{q}^{(3)}, \dots, \mathbf{q}^{(\xi)}$ are linearly independent and hence $\eta(G') \geq \eta(G'')$. Theorem 6 implies $\eta(G') \leq \eta(G'')$. It follows that $\eta(G') = \eta(G'')$, as claimed.

Iteration of Theorem 14 gives directly:

Corollary 15. Let G be a graph and H an attachment set. Then

$$\eta(\mathfrak{a}(G,H)) = \eta(\mathfrak{a}^n(G,H)) \tag{20}$$

for any $n \geq 1$.

Hence, successive altanisations surround the original patch and its first-altan penumbra of faces with rings of h hexagons, but do not change the nullity of the graph. Given the restrictive range of bond lengths available to carbon nanostructures, this implies that at some level of iterated altanisation the system will pop out of the plane and form a tube-like structure, closed at one end by the patch and its first altan acting together as a generalised hemispherical cap. This change in geometrical structure has implications for the chemistry of any such molecule (see Section 7).

4 Computational results

The preceding sections have presented mathematical theorems for the limits on excess nullity. The excess can take values 0, 1 or 2 only. It is of interest to check how these cases are distributed for examples of chemical relevance. We made a computational survey of small examples, to get some information about the relative frequencies of the different allowed values. The chosen families of molecular graphs are benzenoids (general, catafused and convex) and patches composed of various combinations of 5-, 6- and 7-membered rings (solely pentagonal, solely heptagonal, pentagonal-and-hexagonal and pentagonal-and-heptagonal).

General and catacondensed benzenoids were generated using the catacondensed generator which is included in the CaGe package [53]. For convex benzenoids we used in-house software that was developed for stratified enumeration reported in [54]. The ngons generator from the CaGe package was used for the other families of patches. To determine nullity of parent and altan graphs we developed a program in SageMath [55] that uses the rank method for matrices over the integer ring (exact linear algebra computation). Calculations are carried out for the natural attachment set only. Calculations of the altan nullity are needed only for patches with (natural) attachment sets of even size, as odd attachment sets give trivially zero excess nullity (Corollary 12).

Table 1 presents the results for benzenoids on up to 15 hexagons. Table 2 shows the results for the equivalent computation limited to the catafused benzenoids. The most striking conclusion from both tables is that by far the majority of altan benzenoids have minimum excess nullity (i.e. 1 for Kekulean benzenoids and 0 for non-Kekulean benzenoids). Cases with the next allowed value soon start to appear, and of these the most interesting is for Kekulean (i.e. non-singular) benzenoid parents that give rise to altans with nullity 2. As mentioned earlier, this possibility had not been noticed before. Here we see that it occurs for benzenoids with 5 and 7 hexagons, and then, apparently, for all numbers of hexagons from 9 on. Figure 8 shows the smallest examples of catafused and perifused benzenoids for which the nullity jumps by two on altanisation. Figure 9 shows the smallest examples for which the nullity jumps by two for non-Kekulean benzenoids.

If we limit consideration to the subclass of convex benzenoids [51], we can readily take the analysis much further, and Table 3 shows the results for cases with up to 3000 hexagons. In all the 760511 examples included in this survey, the excess nullity is either 0 or 1. The paractical chemical consequence is clear. This exhaustive computation rules out the possibility that an altan of a convex benzenoid (which, as noted above, contains faces of length 5 and 6 only) will be found in small-molecule synthetic chemistry. It also makes it tempting to make the conjecture that no convex benzenoid has excess nullity 2, and in particular that no Kekulean convex benzenoid has an altan with nullity 2. We have developed a proof strategy for this conjecture, but for reasons of space we do not give it here. The proof will be reported in full elsewhere. We also note that within the range of computations, excess nullity of 1 in Table 3 is in fact found for parent nullities of 0 or 2 only, even though parents with higher nullities occur.

Benzenoids, as bipartite patches, have a strong connection between nullity of the parent patch and the size of its natural attachment set, as made explicit in Corollary 3. This connection is broken for more general patches in which some faces are odd, and in particular for the pentagonal, heptagonal and mixed pentagon/hexagon patches treated in Tables 4, 5 and 6. In these cases, the results for small numbers of faces and natural attachment sets

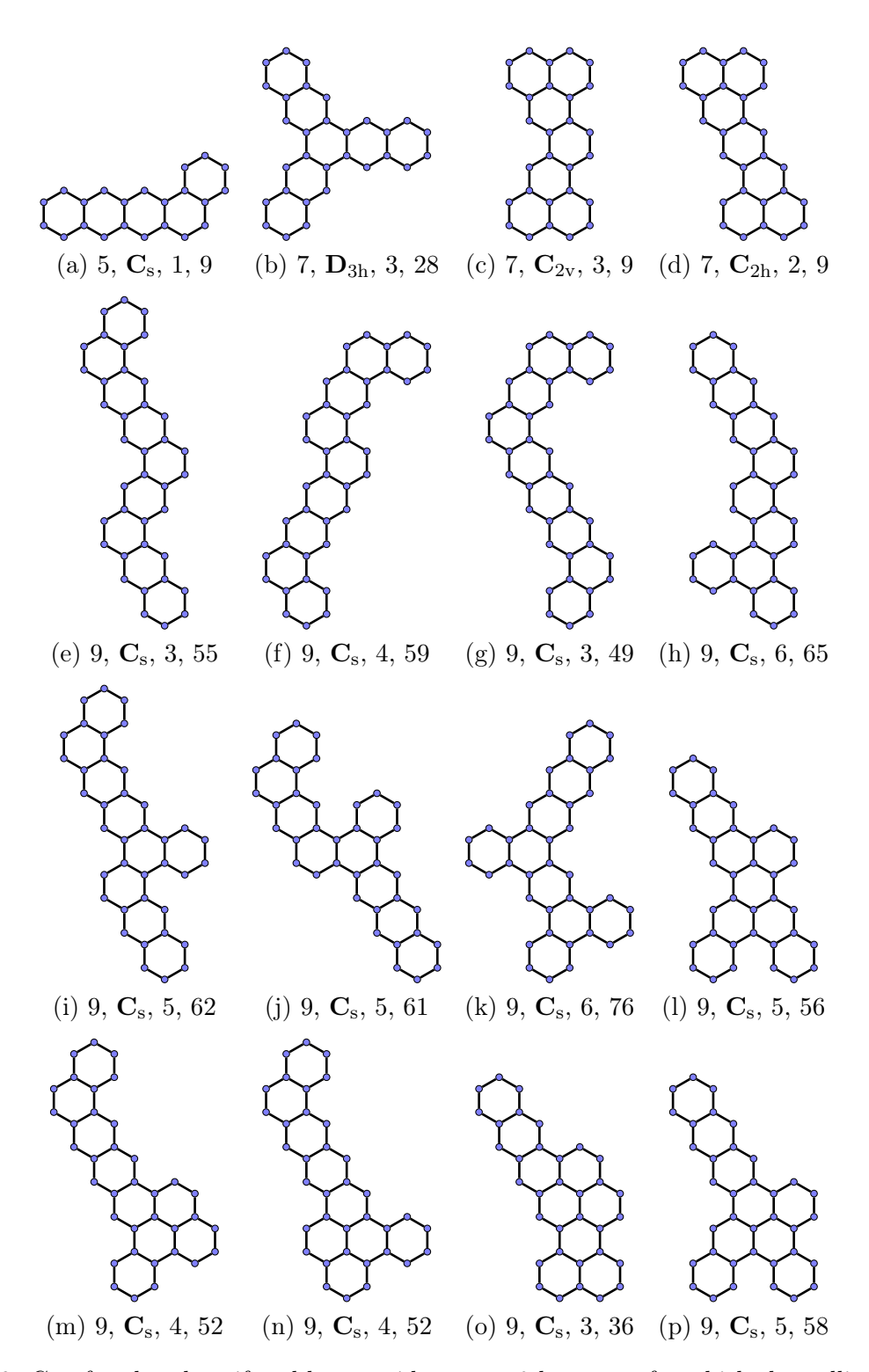


Figure 8: Catafused and perifused benzenoids on $\varepsilon \leq 9$ hexagons for which the nullity jumps from 0 to 2 on altanisation. The subcaption for each benzenoid lists: the number of hexagons, the maximum point group, the bay number and the number of perfect matchings.

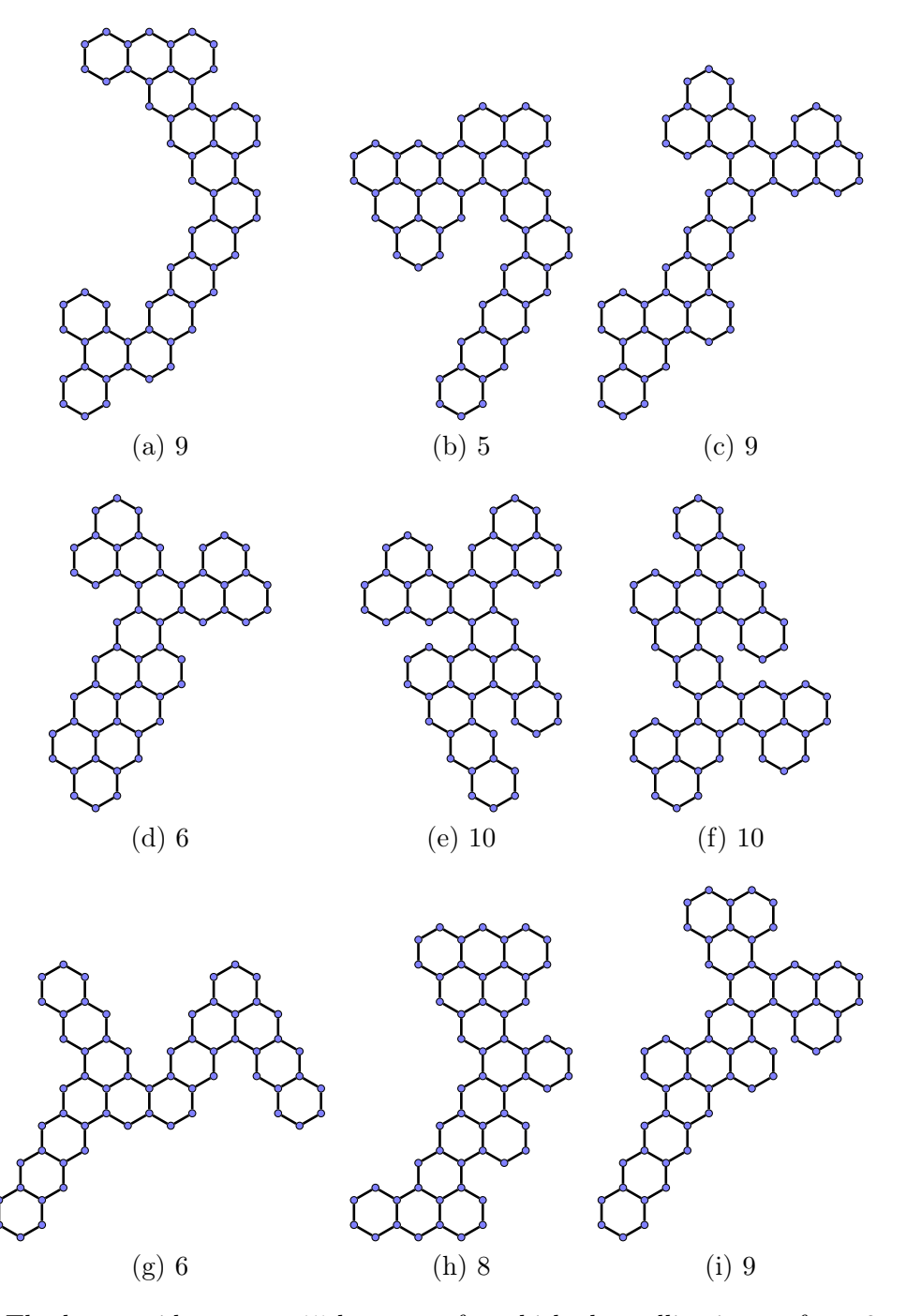


Figure 9: The benzenoids on $\varepsilon=15$ hexagons for which the nullity jumps from 2 to 4 on altanisation. The subcaption for each benzenoid gives the bay number. All of them have the trivial maximum point group \mathbf{C}_{s} .

of even size again show the tendency for the altans with the lowest possible excess nullity to predominate, but the cases with excess nullity 2 appear to be more common than for benzenoids. The pent-hex patches include examples that appear as induced subgraphs in fullerenes [46,47,56], and the class as a whole exhibits richer behaviour than the all-hexagon benzenoids. Some examples indicating the richer behaviour of the non-benzenoid patches are illustrated in Figures 10 and 11.

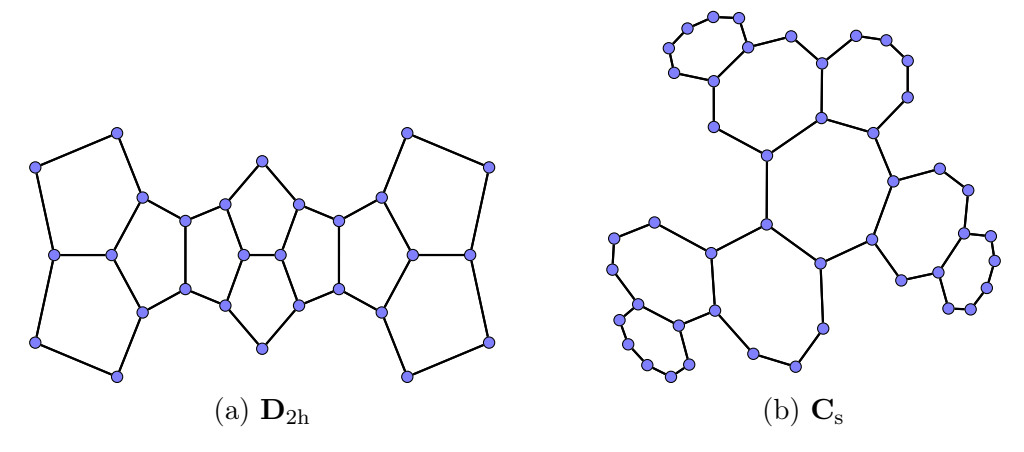


Figure 10: Smallest patches with nullity combination $\eta(\Pi) = 1$, $\eta(\mathfrak{a}(\Pi)) = 3$, which cannot occur for benzenoids: (a) a pure pentagonal patch with 10 pentagons; (b) a pure heptagonal patch with 9 heptagons.

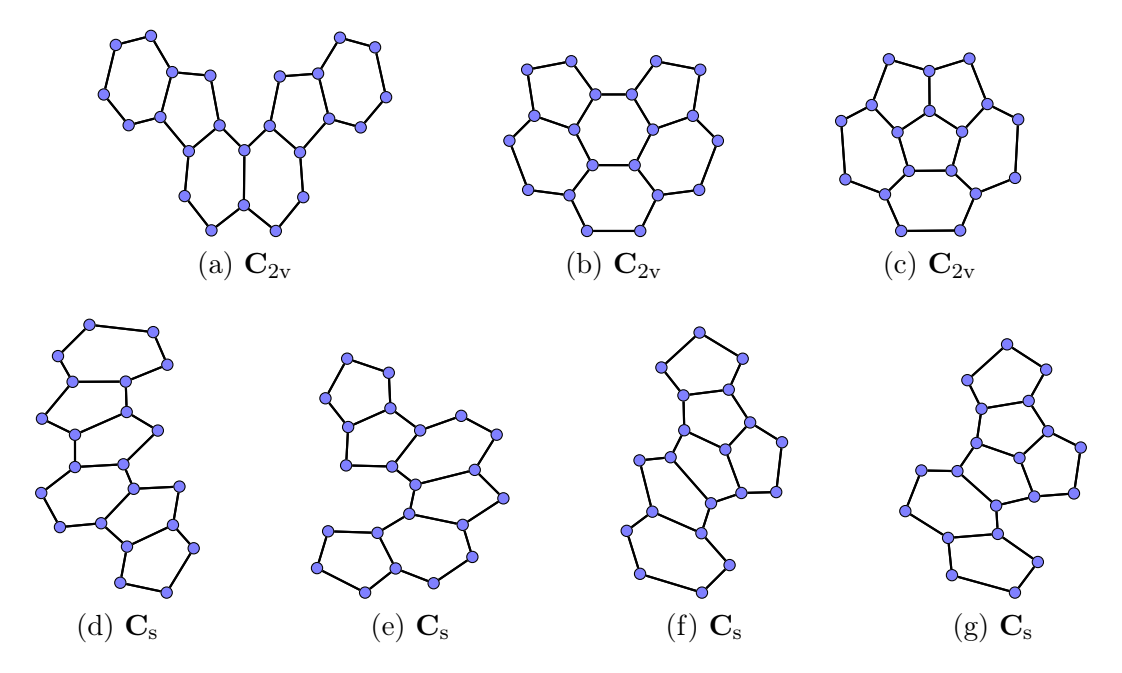


Figure 11: Smallest pent-hex patches with excess nullity $\eta(\mathfrak{a}(\Pi)) - \eta(\Pi) = 2$. All patches have six faces and are shown in the order in which they occur in Table 6.

$\eta(B)$	0	0	2	2	2	4	4	1	3	5
$\eta(\mathfrak{a}(B))$	1	2	2	3	4	4	5	1	3	5
ε 1	1									
2	1									
3	2							1		
4	6							1		
5	14	1						7		
6	51		1	1				28		
7	187	3	7					134		
8	764		51	1				619		
9	3211	12	318	4				2957	3	
10	14073	34	1913	3				14024	39	
11	62782	97	10916	14				67046	374	
12	284552	366	60760	43		14		320859	2990	
13	1303460	1401	331219	116		211		1540174	21675	
14	6026901	4741	1778968	461		2587	1	7408359	145559	
15	28066662	15891	9447084	1589	9	25084		35721421	930122	48

Table 1: Excess nullity for altan-benzenoids based on natural attachment sets. Notation: $\eta(B)$ is the nullity of the parent, $\eta(\mathfrak{a}(B))$ is the nullity of its altan, and ε is the number of hexagons in the parent. The columns display the counts of cases with a given $(\eta(B), \eta(\mathfrak{a}(B)))$ pair. Double vertical lines separate cases with even and odd attachment sets.

$\eta(B)$	0	0
$\eta(\mathfrak{a}(B))$	1	2
ε 1		
2	1	
3	2	
4	5	
5	11	1
6	36	
7	117	1
8	411	
9	1482	7
10	5560	12
11	21090	25
12	81067	54
13	313933	142
14	1224021	507
15	4798445	760
16	18894445	2536

Table 2: Excess nullity for altans of catafused benzenoids. Notation as in Table 1.

$\eta(B)$	odd	even	0	2
$\eta(\mathfrak{a}(B))$	$\eta(B)$	$\eta(B)$	1	3
ε 10	6	1	17	1
20	23	8	43	2
30	49	24	77	2
40	85	44	115	3
50	131	73	157	3
60	184	109	204	4
70	245	153	255	4
80	320	201	308	4
90	401	260	365	5
100	486	324	425	5
200	1842	1374	1150	7
300	4042	3160	2073	9
400	7039	5692	3152	11
500	10853	8968	4359	12
600	15485	13006	5697	13
700	20924	17767	7135	14
800	27146	23295	8675	15
900	34182	29599	10320	16
1000	41993	36603	12032	17
2000	163687	148394	33381	25
3000	364019	335729	60732	31

Table 3: Excess nullity for altans of convex benzenoids. Notation as in Table 1. The entries in each row display cumulative counts of convex benzenoids on up to ε hexagons that have respectively odd attachment set, even attachment set with excess nullity 0, and, after the double vertical lines, nullities 0 and 2 with excess nullity 1.

$\eta(\Pi)$	0	0	1	1	1	2	2	2	3	3	3	4
$\eta(\mathfrak{a}(\Pi))$	1	2	1	2	3	2	3	4	3	4	5	4
π 2				1								
3	1											
4	3											
5	3											
6	7		2	1		1						
7	13		4									
8	36	4	5	1		1						
9	99	1	7									
10	241	3	13	5	1		1					
11	636	2	38	10		1						1
12	1614	16	90	35	1							
13	4363	43	214	38	1	5						
14	11796	78	483	86	3	9						
15	31415	175	1269	176	1	6	1		1			
16	85773	467	3682	532	6	55	2		1			
17	230077	891	9816	1335	10	171	2		2			
18	634433	2757	27844	3166	29	450	15	1	7			
19	1726528	7111	74818	8452	74	1019	13		9			
20	4775761	15562	206502	21357	184	3042	45	4	22			

Table 4: Excess nullity for altans of pure pentagonal patches. Notation: $\eta(\Pi)$ is the nullity of the parent, $\eta(\mathfrak{a}(\Pi))$ is the nullity of its altan, and π is the number of pentagons in the parent. The columns display the counts of cases with a given $(\eta(\Pi), \eta(\mathfrak{a}(\Pi)))$ pair. Only those patches with even h are included in the table.

$\eta(\Pi)$	0	0	1	1	1	2	2	2	3	3	3
$\eta(\mathfrak{a}(\Pi))$	1	2	1	2	3	2	3	4	3	4	5
σ 2			1								
3	1										
4	8										
5	14										
6	131	3	20	7		1					
7	520	2	76	11							
8	5140	24	480	77		2	2				
9	28326	114	2107	268	1	29					
10	235776	907	19021	2401	5	327	2		5	3	
11	1506162	3912	121424	14523	46	2589	17		11		
12	12006702	26415	982165	112734	242	19050	285	3	263	2	

Table 5: Excess nullity for altans of pure heptagonal patches. The number of heptagons is denoted σ and all other notation is as in Table 4. Only those patches with even h are included in the table.

$\eta(\Pi)$			0	0	1	1	1	2	2	2
$\eta(\mathfrak{a}(I))$	I))		1	2	1	2	3	2	3	4
π, ε	1	2	1							
	2	1	2			1				
	1	3	4							
	2	2	12		1	3				
	3	1	3							
	1	4	25							
	2	3	67		2	3				
	3	2	32		2					
	4	1	21			1				
	1	5	132							
	2	4	378	2	11	2	1			
	3	3	257	1	8	1				
	4	2	206	2	6	3				
	5	1	43	2	1					
	1	6	722							
	2	5	2092	1	45	8				
	3	4	1987	3	64	5				
	4	3	1765	8	40	7	1			
	5	2	643	3	11	2				
	6	1	158	1	12	1	1			
	1	7	3865	11	4	1				
	2	6	11987	14	234	17		9		
	3	5	14290	22	386	27				
	4	4	14759	29	260	28	1			
	5	3	7272	9	109	7				
	6	2	2587	16	94	14	1	1		
	7	1	445	3	29	4		1		
	1	8	20867	43	66	9		28		
	2	7	68824	31	1289	76		105	1	
	3	6	99388	84	2447	127				
	4	5	115988	122	1719	129				
	5	4	72812	106	961	62		3		
	6	3	33541	74	651	59	1	2		
	7	2	8917	18	340	29		3		
	8	1	1337	11	70	13				

Table 6: Excess nullity for altans of mixed pent-hex patches. The numbers of pentagons and hexagons are denoted π and ε , respectively. All other notation is as in Table 4. Only those patches with even h are included in the table.

5 Relationship to previous work

The theorems in Section 3 allow some comment on previous work on the systematics of altanisation. Various observations made in the chemical literature on altanisation and the number of non-bonding orbitals were generalised and put into a formal mathematical framework in two papers by Gutman [32,33] and have been taken up again in a recent paper by Dickens and Mallion on the predicted magnetic response properties of altans [31].

The paper [32] concentrates on altans of benzenoids, and gives a number of rules for the face sizes, perimeter length, Kekulé count, and numbers of NBMOs. Of these, one requires a change in the light of Theorem 7. Rule 7 [32] states that "Altan-benzenoid hydrocarbons have NBMOs. Kekulean altan-benzenoids have a unique NBMO." Unique NBMOs are illustrated for two small cases in an accompanying figure. However, a Kekulean benzenoid has nullity zero, and therefore the present Theorem 7 also allows the existence of altans of Kekulean benzenoids that have nullity two (but no more). The case illustrated in the present Figure 6 in fact exhibits nullity two, so the second part of Rule 7 should be amended to "Kekulean altan-benzenoids can have either one or two independent NBMOs." The 'unique' NBMO referred to in [32] is our 'special one', but as we have shown there can be an additional NBMO in some cases.

The second paper [33] generalises the theory to altans of general graphs, and gives key definitions that we have followed here. Salient results given as Theorems and Corollaries include a prior proof of Theorem 5. Some confusion has arisen in later work [31] between proven results from [33] and some cases that were being quoted there merely as examples. In Corollary 11 of [33] (which refers to cases with even h = |H|) it is noted that "The case $\eta(G^{\dagger}) = \eta(G) + 1$ is encountered if G is non-singular." (In our notation, G^{\dagger} would be $\mathfrak{a}(G, H)$.) The statement does not exclude the possibility of other values of $\eta(G^{\dagger})$ being encountered, nor does it imply anything about singular graphs G. The reading that led to the tentative proposal in [31] of a possible general rule of increase of nullity by 1 for an altan of any G, is therefore not correct. Indeed, that proposal runs into a contradiction when G is itself an altan, as the authors themselves notice, and has many exceptions even for non-altan G, as our tables show.

6 Chemical implications

To be concrete, our present understanding of the relations between the numbers of NBMOs predicted by Hückel Theory for a parent hydrocarbon and its successive altans, assuming separate σ and π structures, can be summarised in a short set of chemical rules. Let η and $\eta(\mathfrak{a})$ be the numbers of NBMOs of the parent and altan respectively, and h be the number of sp^2 CH sites on the perimeter of the parent molecule (the natural attachment set). Then:

- (i) If h is odd, the number of π NBMOs is the same for the parent and the first and all subsequent iterated altans.
- (ii) If h is even, the number of π NBMOs in the first altan has one of the three values, $\eta(\mathfrak{a}) = \eta$ or $\eta + 1$ or $\eta + 2$, subject to the proviso that if $\eta = 0$, the altan has $\eta(\mathfrak{a}) = 1$ or 2. All subsequent altans of the given parent have the same number of π NBMOs as the first.

- (iii) For the important specific case of a Kekulean benzenoid parent, for which the natural attachment set necessarily has even size and the nullity is $\eta = 0$, the rule is that $\eta(\mathfrak{a}) = 1$ or 2, and all iterated altans have $\eta(\mathfrak{a}) \pi$ NBMOs.
- (iv) Likewise, for a non-Kekulean benzenoid parent with odd nullity, the parent, first altan and all iterated altans have the same number of π NBMOs. For a non-Kekulean benzenoid parent with even nullity, the nullity may increase (by at most 2) on first altanisation, but then remains constant for all further iterated altans.
- (v) Finally, for the class of convex benzenoids, the conjecture, based on extensive computation, is that $\eta(\mathfrak{a})$ in these cases is η or $\eta+1$. For odd h, $\eta(\mathfrak{a})=\eta$. The conjecture implies that the altan of a Kekulean convex benzenoid has $\eta=1$. Notwithstanding any proof or disproof, exhaustive calculations show that there are no exceptions with fewer than 3000 hexagonal rings.

Two caveats about the applicability of these rules are in order. Chemists will want to bear in mind that the rules are derived within the Hückel model for planar systems, as noted in the preamble. The first is that when h is even, they only give bounds on $\eta(\mathfrak{a})$. Those bounds are strict, but they still allow a small range of values. As the proof strategies used in Section 3 show, the occurrence of the more unusual (i.e. higher) values of the difference $\eta(\mathfrak{a}) - \eta$ can be traced back to specific properties of the NBMOs of the parent graph. So far, we have not attempted to give a complete characterisation of all such cases, though this would be an interesting direction for future research.

7 Conclusion

This paper has given some precise theorems about the spectra of altan graphs. To assess their chemical significance, several factors must be considered.

The Hückel model itself is clearly a relatively crude model for planar or nearly planar π systems. Ordering of orbital energies may change with geometric factors, total charge, or increase in the level of theory and use of calculations based on more sophisticated quantum chemical methods.

For example, the assumptions of Hückel theory in its simplest form, that resonance integrals for all bonded pairs are equal and that Coulomb integrals for all carbon centres are equal, will become less appropriate for the geometrically non-planar structures produced by iterated altanisation, and they may be expected to exhibit local differences in reactivity and changes in overall stability, as occur for example in fullerenes [57].

Even within the Hückel regime appropriate to geometrically planar systems, there may be little practical difference between zero and near-zero graph eigenvalues (between non-bonding and very weakly bonding or antibonding orbitals). The crowding of the entire spectrum of a chemical graph into the open interval between +3 and -3 suggests that large graphs, such as those produced by iterated altanisation may typically have several eigenvalues of very small magnitude that are not detected by the rules for counting strict zeroes but may have a similar impact on molecular properties.

Finally, the chemical significance of a non-bonding orbital depends to an extent on the position of the zero eigenvalue within the the ordered graph spectrum. Hückel Theory is

acknowledged to perform at its best when applied to neutral or near-neutral systems, where the numbers of positive and negative eigenvalues are both close to n/2. If an NBMO occurs too early or too late in the order, its properties are less likely to be relevant to physically realistic descriptions of the system. Nevertheless, having precise rules for the number of such orbitals is a useful first step in building qualitative models of stability, reactivity and magnetic response.

Acknowledgements

The work of Nino Bašić is supported in part by the Slovenian Research Agency (Research Programme P1-0294 and Research Projects J1-9187, J1-1691, N1-0140 and J1-2481). PWF thanks the Leverhulme Trust for an Emeritus Fellowship on the theme of 'Modelling molecular currents, conduction and aromaticity'.

ORCID iDs

Nino Bašić https://orcid.org/0000-0002-6555-8668 Patrick W. Fowler https://orcid.org/0000-0003-2106-1104

References

- [1] P. von Ragué Schleyer (Guest Ed.), Aromaticity [Special Issue], *Chem. Rev.* **101** (2001), 1115–1566.
- [2] P. von Ragué Schleyer (Guest Ed.), Delocalization—Pi and Sigma [Special Issue], *Chem. Rev.* **105** (2005), 3433–3947.
- [3] N. Martín and L. T. Scott (Guest Eds), Challenges in aromaticity: 150 years after Kekulé's benzene [Themed Collection], Chem. Soc. Rev. 44 (2015), 6397–6643.
- [4] M. Rickhaus, M. Jirásek, L. Tejerina, H. Gotfredsen, M. D. Peeks, R. Haver, H.-W. Jiang, T. D. W. Claridge and H. L. Anderson, Global aromaticity at the nanoscale, *Nat. Chem.* 12 (2020), 236–242, doi:10.1038/s41557-019-0398-3.
- [5] M. Jirásek, H. L. Anderson and M. D. Peeks, From macrocycles to quantum rings: Does aromaticity have a size limit?, *Acc. Chem. Res.* **54** (2021), 3241–3251, doi:10.1021/acs. accounts.1c00323.
- [6] F. London, Théorie quantique des courants interatomiques dans les combinaisons aromatiques, J. Phys. Radium 8 (1937), 397–409, doi:10.1051/jphysrad:01937008010039700.
- J. A. Pople, Molecular orbital theory of aromatic ring currents, Mol. Phys. 1 (1958), 175–180, doi:10.1080/00268975800100211.
- [8] R. McWeeny, Ring currents and proton magnetic resonance in aromatic molecules, *Mol. Phys.* **1** (1958), 311–321, doi:10.1080/00268975800100381.

- [9] P. von Ragué Schleyer and H. Jiao, What is aromaticity?, Pure Appl. Chem. 68 (1996), 209–218, doi:10.1351/pac199668020209.
- [10] G. Monaco and R. Zanasi, Three contra-rotating currents from a rational design of polycyclic aromatic hydrocarbons: altan-corannulene and altan-coronene, *J. Phys. Chem. A* **116** (2012), 9020–9026, doi:10.1021/jp302635j.
- [11] M. Stępień, An aromatic riddle: Decoupling annulene conjugation in coronoid macrocycles, *Chem* 4 (2018), 1481–1483, doi:10.1016/j.chempr.2018.06.008.
- [12] W. E. Barth and R. G. Lawton, Synthesis of corannulene, J. Am. Chem. Soc. 93 (1971), 1730–1745, doi:10.1021/ja00736a028.
- [13] G. Ege and H. Vogler, Zur Konjugation in makrocyclischen Bindungssystemen XX. Charakterordnung, magnetische Suszeptabilitäten und chemische Verschiebungen von Corannulenen, *Theor. Chim. Acta* **26** (1972), 55–65, doi:10.1007/bf00527653.
- [14] F. Diederich and H. A. Staab, Benzenoid versus annulenoid aromaticity: synthesis and properties of kekulene, Angewandte Chemie - International Edition in English 17 (1978), 372–374, doi:10.1002/anie.197803721.
- [15] J. Aihara, Validity and limitations of the annulene-within-an-annulene (awa) model for macrocyclic π-systems, RSC Adv. 4 (2014), 7256–7265, doi:10.1039/c3ra45874a.
- [16] E. Steiner, P. W. Fowler and L. W. Jenneskens, Counter-rotating ring currents in coronene and corannulene, Angew. Chem. Int. Ed. 40 (2001), 362–366, doi:10.1002/1521-3773(20010119)40:2<362::aid-anie362>3.3.co;2-q.
- [17] G. Monaco, R. G. Viglione, R. Zanasi and P. W. Fowler, Designing ring-current patterns: [10,5]-coronene, a circulene with inverted rim and hub currents, *J. Phys. Chem. A* **110** (2006), 7447–7452, doi:10.1021/jp0600559.
- [18] G. Monaco, P. W. Fowler, M. Lillington and R. Zanasi, Designing paramagnetic circulenes, *Angew. Chem. Int. Ed.* 46 (2007), 1889–1892, doi:10.1002/ange.200604261.
- [19] E. Steiner, P. W. Fowler and L. W. Jenneskens, Counter-rotating ring currents in coronene and corannulene, *Angew. Chem. Int. Ed.* **40** (2001), 362–366, doi:10.1002/1521-3773(20010119)40:2<362::aid-anie362>3.0.co;2-z.
- [20] G. Monaco, M. Memoli and R. Zanasi, Additivity of current density patterns in altanmolecules, J. Phys. Org. Chem. 26 (2013), 109–114, doi:10.1002/poc.2958.
- [21] R. Zanasi, P. Della Porta and G. Monaco, The intriguing class of altan-molecules, *J. Phys. Org. Chem.* **29** (2016), 793–798, doi:10.1002/poc.3558.
- [22] G. Monaco and R. Zanasi, Anionic derivatives of altan-corannulene, J. Phys. Org. Chem. **26** (2013), 730–736, doi:10.1002/poc.3117.
- [23] T. K. Dickens and R. B. Mallion, Ring-current assessment of the annulene-within-an-annulene model for some large coupled super-ring conjugated-systems, *Croat. Chem. Acta* 87 (2014), 221–232, doi:10.5562/cca2397.

- [24] T. K. Dickens and R. B. Mallion, π -electron ring-currents and bond-currents in some conjugated altan-structures, *J. Phys. Chem. A* **118** (2014), 3688–3697, doi:10.1021/jp502585f.
- [25] T. K. Dickens and R. B. Mallion, Topological Hückel-London-Pople-McWeeny ring currents and bond currents in altan-corannulene and altan-coronene, *J. Phys. Chem. A* 118 (2014), 933–939, doi:10.1021/jp411524k.
- [26] T. K. Dickens and R. B. Mallion, Topological ring-currents and bond-currents in the altan-[r,s]-coronenes, *Chem. Commun.* **51** (2015), 1819–1822, doi:10.1039/c4cc07322c.
- [27] T. K. Dickens and R. B. Mallion, Topological ring-current and bond-current properties of the altans of certain K-factorizable conjugated systems containing "fixed" single-bonds, *J. Phys. Chem. A* **119** (2015), 5019–5025, doi:10.1021/acs.jpca.5b02826.
- [28] T. K. Dickens and R. B. Mallion, Topological ring currents and bond currents in some neutral and anionic altans and iterated altans of corannulene and coronene, J. Phys. Chem. A 122 (2018), 7666–7678, doi:10.1021/acs.jpca.8b06862.
- [29] M. Piccardo, A. Soncini, P. W. Fowler, G. Monaco and R. Zanasi, Design of annulene-within-an-annulene systems by the altanisation approach. a study of altan-[n]annulenes, *Phys. Chem. Chem. Phys.* 22 (2020), 5476–5486, doi:10.1039/c9cp06835j.
- [30] T. K. Dickens and R. B. Mallion, Topological ring-currents and bond-currents in hexaanionic altans and iterated altans of corannulene and coronene, *J. Phys. Chem. A* **124** (2020), 7973–7990, doi:10.1021/acs.jpca.0c04606.
- [31] T. K. Dickens and R. B. Mallion, Topological ring currents and bond currents in neutral and dianionic altans and iterated altans of benzene, naphthalene, and azulene, *J. Phys. Chem. A* **125** (2021), 10485–10499, doi:10.1021/acs.jpca.1c07846.
- [32] I. Gutman, Topological properties of altan-benzenoid hydrocarbons, J. Serbian Chem. Soc. **79** (2014), 1515–1521, doi:10.2298/jsc140619080g.
- [33] I. Gutman, Altan derivatives of a graph, *Iranian J. Math. Chem.* **5** (2014), 85–90, doi: 10.22052/ijmc.2014.6127.
- [34] N. Bašić and T. Pisanski, Iterated altans and their properties, MATCH Commun. Math. Comput. Chem. 74 (2015), 645–658.
- [35] N. Bašić, P. W. Fowler and T. Pisanski, Coronoids, patches and generalised altans, J. Math. Chem. 54 (2016), 977–1009, doi:10.1007/s10910-016-0599-6.
- [36] N. Trinajstić, *Chemical Graph Theory*, Mathematical Chemistry Series, CRC Press, Boca Raton, FL, 2nd edition, 1992, doi:10.1007/s10910-008-9464-6.
- [37] I. Gutman, Computing the dependence of graph energy on nullity: the method of siblings, Discrete Math. Lett. 7 (2021), 30–33, doi:10.47443/dml.2021.0038, https://doi.org/ 10.47443/dml.2021.0038.
- [38] I. Gutman, Graph energy and nullity, Open J. Discrete Appl. Math. 4 (2021), 25–28.

- [39] I. Gutman and I. Triantafillou, Dependence of graph energy on nullity: a case study, MATCH Commun. Math. Comput. Chem. **76** (2016), 761–769.
- [40] D. M. Cvetković, M. Doob and H. Sachs, Spectra of Graphs: Theory and Applications, Johann Ambrosius Barth, Heidelberg, 3rd edition, 1995.
- [41] A. E. Brouwer and W. H. Haemers, *Spectra of Graphs*, Universitext, Springer, New York, 2012, doi:10.1007/978-1-4614-1939-6.
- [42] D. M. Cvetković, P. Rowlinson and S. Simić, Eigenspaces of Graphs, volume 66 of Encyclopedia of Mathematics and its Applications, Cambridge University Press, Cambridge, 1997, doi:10.1017/cbo9781139086547.
- [43] D. M. Cvetković, P. Rowlinson and S. Simić, An introduction to the theory of graph spectra, volume 75 of London Mathematical Society Student Texts, Cambridge University Press, Cambridge, 2010.
- [44] F. R. K. Chung, Spectral Graph Theory, volume 92 of CBMS Regional Conference Series in Mathematics, American Mathematical Society, Providence, RI, 1997.
- [45] I. Gutman and B. Borovićanin, Nullity of graphs: an updated survey, Zb. Rad. (Beogr.) 14(22) (2011), 137–154.
- [46] J. E. Graver and C. M. Graves, Fullerene patches I, Ars Math. Contemp. 3 (2010), 109–120, doi:10.26493/1855-3974.135.29d.
- [47] J. E. Graver, C. Graves and S. J. Graves, Fullerene patches II, Ars Math. Contemp. 7 (2014), 405–421, doi:10.26493/1855-3974.391.a0d.
- [48] D. J. Klein and A. T. Balaban, The eight classes of positive-curvature graphitic nanocones, J. Chem. Inf. Model. 46 (2006), 307–320, doi:10.1021/ci0503356.
- [49] G. Brinkmann, O. Delgado-Friedrichs and U. von Nathusius, Numbers of faces and boundary encodings of patches, in: *Graphs and Discovery*, Amer. Math. Soc., Providence, RI, volume 69 of *DIMACS Ser. Discrete Math. Theoret. Comput. Sci.*, pp. 27–38, 2005, doi:10.1090/dimacs/069/03, https://doi.org/10.1090/dimacs/069/03.
- [50] I. Gutman and S. J. Cyvin, *Introduction to the Theory of Benzenoid Hydrocarbons*, Springer-Verlag, Berlin, 1989.
- [51] R. Cruz, I. Gutman and J. Rada, Convex hexagonal systems and their topological indices, MATCH Commun. Math. Comput. Chem. 68 (2012), 97–108.
- [52] G. Monaco, On the diatropic perimeter of iterated altan-molecules, *Physical Chemistry Chemical Physics* **17** (2015), 28544–28547, doi:10.1039/c5cp05520b.
- [53] G. Brinkmann, O. Delgado Friedrichs, S. Lisken, A. Peeters and N. Van Cleemput, CaGe—a virtual environment for studying some special classes of plane graphs—an update, MATCH Commun. Math. Comput. Chem. 63 (2010), 533–552.

- [54] N. Bašić, P. W. Fowler and T. Pisanski, Stratified enumeration of convex benzenoids, *MATCH Commun. Math. Comput. Chem.* **80** (2018), 153–172.
- [55] The Sage Developers, SageMath, the Sage Mathematics Software System (Version 9.4), 2021, https://www.sagemath.org.
- [56] N. Bašić, G. Brinkmann, P. W. Fowler, T. Pisanski and N. Van Cleemput, Sizes of pentagonal clusters in fullerenes, *J. Math. Chem.* **55** (2017), 1669-1682, doi:10.1007/s10910-017-0754-8.
- [57] P. W. Fowler and D. E. Manolopoulos, *An Atlas of Fullerenes*, Dover, Mineola, New York, 2006.